# On the Charge Regulation of Proteins

Mikael Lund* and Bo Jönsson

*Theoretical Chemistry, Chemical Center, Post Office Box 124, S-221 00 Lund, Sweden*

*Received November 8, 2004; Revised Manuscript Received January 5, 2005*

ABSTRACT: It is known that the overall charge of a protein can change as the molecule approaches a charged object like another protein or a cell membrane. We have formalized this mechanism using a statistical mechanical framework and show how this rather overlooked interaction increases the attraction between protein molecules. From the theory, we can identify a unique property, the *protein charge capacitance*, that contains all information needed to describe the charge regulation mechanism. The capacitance can be obtained from experiment or theory and is a function of pH, salt concentration, and the number of titrating residues. For a range of different protein molecules, we calculate the capacitance and demonstrate how it can be used to quantify the charge regulation interaction. With minimal effort, the derived formulas can be used to improve existing models by including a charge regulation term. Good agreement is found between theory, simulations, and experimental data.

Knowledge of the basic intermolecular interactions between biomolecules is of vital importance for our understanding of processes in the living cell. This includes, for example, the interaction of a protein with small ligands, with DNA, or with a membrane surface, as well as the interaction between two or more protein molecules. The interaction of two proteins, each with a nonzero net charge, is at long distances dominated by a direct Coulomb interaction. The protein charges come from ionized amino acid residues and will vary with pH and other solution conditions. The majority of models presented in the literature describing protein−protein interactions, however, implement the protein charge distribution as a *fixed* set of charges (*1*−*4*) or even by a single-point charge. This is probably still a valid approach for proteins carrying a significant net charge, but when an approximately neutral protein, pH ≈ pI, is approaching a charged surface or another highly charged protein, its charge distribution will change. That is, the protonation state of the protein not only depends on pH but also on nearby molecules; the electrostatic potential from a neighboring molecule will perturb the titrating groups in the protein. This is of course the same effect as is seen internally in a protein, where any charged amino acid may affect the apparent p$K_a$ values of all other groups. Our aim is to formally describe this interaction in mathematical terms and then to numerically calculate the appropriate response function. For the latter, we will use Monte Carlo (MC) simulations describing the protein in atomic detail including all ion−ion interactions within the protein and with the surrounding salt solution.

Charge regulation for colloidal particles has been discussed by Kirkwood and Shumaker (*5*) and later by Carnie et al. (*6*, *7*) within the Debye−Hückel approximation. Zydney et al. have used a similar approach and found the regulation mechanism important for proteins in porous media (*8*), in membranes (*9*), and in capillary electrophoresis experiments (*10*). Bowen and Williams (*11*) solved the Poisson−Boltzmann equation for a sphere in a Wigner−Seitz cell so as to mimic bovine serum albumin. They found that inclusion of a charge regulation term significantly improved the agreement with measured osmotic coefficients. Ståhlberg et al. (*12*−*14*) have studied the net charge of lysozyme in the context of ion-exchange chromatography, where they show how the charge regulation, i.e., the capacitance of a protein, can be derived from the experimental titration curve.

## THEORY AND METHODS

*Protein Charge Capacitance: Statistical Mechanical Derivation.* In this section, we will derive a formal expression for the capacitance in terms of charge fluctations. The essence is captured in eqs 5 and 6, and the reader may want to proceed directly to this part. Let us start by considering two proteins in a salt solution, each described by the charge distributions [$\mathbf{r}_i$, $q_i$] and [$\mathbf{r}_j$, $q_j$], respectively. The mass centra of the distributions are separated by $\mathbf{R}$, which means that the distance between two charges $i$ and $j$ is given by $r_{ij} = |\mathbf{R} + \mathbf{r}_j - \mathbf{r}_i|$. The average net charge number of the distributions does not need to be zero, that is, $\langle Q_A \rangle \neq 0$, where $\langle Q_A \rangle = \langle \sum q_i \rangle$. The free energy of interaction can be written as,

$$\beta A(R) = -\ln\langle e^{-\beta U(R)} \rangle \approx -\ln\left[1 - \langle \beta U(R) \rangle + \frac{1}{2}\langle (\beta U(R))^2 \rangle\right] \quad (1)$$

where $U(R)$ is the interaction between the two charge distributions, $\beta = 1/kT$, with $k$ being the Boltzmann constant and $T$ being the temperature, and $\langle ... \rangle$ denotes an average over the unperturbed system, which in the present case is the single isolated protein in salt solution. The average runs over all orientations and ionization states of the protein as well as over the positions of all salt particles. This means that the calculated averages will depend on both the salt and protein concentrations and pH. Equation 1 can be expanded to a second order as $\ln(1 - x) \approx -x - x^2/2$ for small $x$,

* To whom correspondence should be addressed. Telephone: +46-46-222 0381. Fax: +46-46-222 4543. E-mail: mikael.lund@teokem.lu.se.

10.1021/bi047630o CCC: $30.25 
Published on Web 03/19/2005

$$\beta A(R) \approx \langle \beta U(R) \rangle - \frac{1}{2}[\langle (\beta U(R))^2 \rangle + \langle \beta U(R) \rangle^2] \quad (2)$$

The interaction energy is simply the Coulomb interaction between the two charge distributions,

$$\beta U(R) = \sum_i \sum_j \frac{l_B q_i q_j}{r_{ij}} \quad (3)$$

where the Bjerrum length, $l_B = e^2/4\pi\epsilon_0\epsilon_r kT$ has been introduced. We can make a multipole expansion of the energy, assuming that $R \gg r_i, r_j$. This expansion will include an ion−ion interaction, an ion−dipole interaction, a dipole−dipole interaction, etc. It will also include charge-induced charge and induced charge-induced charge interactions. Thus, we can write an approximation to the free energy including all terms of order up to $1/R^2$. Note that the ion−dipole interaction disappears in the first order and that the first nonvanishing dipole term will be of the order $1/R^4$.

$$\beta A(R) \approx \frac{l_B \langle Q_A \rangle \langle Q_B \rangle}{R} - \frac{l_B^2}{2R^2}[\langle Q_A^2 \rangle \langle Q_B^2 \rangle - \langle Q_A \rangle^2 \langle Q_B \rangle^2] \quad (4)$$

Note also that $\langle Q^2 \rangle \neq \langle Q \rangle^2$. We now define a "charge polarizability" or capacitance, $C$, that quantifies the charge fluctuations of the protein,

$$C \equiv \langle Q^2 \rangle - \langle Q \rangle^2 = -\frac{\partial Q}{\partial \beta e \Phi} \quad (5)$$

where linear response theory gives the relation to the electrical potential, $\Phi$. With this definition of the capacitance, eq 4 can be rewritten in a more useful form,

$$\beta A(R) \approx \frac{l_B \langle Q_A \rangle \langle Q_B \rangle}{R} - \frac{l_B^2}{2R^2}(C_A C_B + C_A \langle Q_B \rangle^2 + C_B \langle Q_A \rangle^2) \quad (6)$$

The first term is the direct Coulomb term, and the following terms are the *induced charge-induced charge* and *charge-induced charge* interactions. If the protein molecules are identical, that is, $\langle Q_A \rangle = \langle Q_B \rangle = \langle Q \rangle$, the expression then simplifies to,

$$\beta A(R) \approx \frac{l_B \langle Q \rangle^2}{R} - \frac{l_B^2}{2R^2}(C^2 + 2C\langle Q \rangle^2) \quad (7)$$

and if the proteins happen to be at pH = pI, then $\langle Q \rangle = 0$ and the leading term is the induced charge-induced charge interaction,

$$\beta A(R) \approx -\frac{l_B^2 C^2}{2R^2} \quad (8)$$

which is equivalent to the findings of Bratko et al. (*15*) for the intermolecular interaction between micelles subject to charge fluctuations of the number of counterions.

The above equations show that the fluctuating charge of a protein may under certain circumstances contribute significantly to the net interaction between two proteins. From eq 5, we can also write the induced charge as $Q_{ind} = -C\beta e \Delta\Phi$, valid for small potentials. Note that in the derived equations we have used an unscreened Coulomb potential (eq 3) valid for no or very low salt concentrations, only. To include the effect of salt, it is necessary to use a screened potential; an example of this is shown in eq 14.

*Macroscopic Picture.* The capacitance, $C$, can be derived from the protein titration curve. For a single titrating acid, the degree of ionization, α, can be found in any elementary physical chemistry textbook,

$$\mathrm{pK} = \mathrm{pH} - \log\frac{\alpha}{1-\alpha} \quad (9)$$

Taking the derivative of α with respect to pH gives

$$\frac{\partial \alpha}{\partial \mathrm{pH}} = \alpha(1-\alpha)\ln 10 = C \ln 10 \quad (10)$$

where in the second step we have identified the capacitance defined in eq 5. We can obtain an approximate value for the capacitance in a protein assuming that there is no interaction between the titrating sites: A protein contains several titrating groups such as aspartic and glutamic acid, histidine, etc., each with an ideal p$K_0$ value. When different titrating groups are denoted with $\gamma$ and their number with $n_\gamma$, the total capacitance can then be approximated with,

$$C^{ideal} = \sum_\gamma n_\gamma \frac{10^{\mathrm{pH}-\mathrm{pK}_{0,\gamma}}}{(1+10^{\mathrm{pH}-\mathrm{pK}_{0,\gamma}})^2} \quad (11)$$

More realistic capacitances, where intramolecular interactions are included, can be obtained from experimental protein titration curves, readily available in the literature. As evident from eq 10, the capacitance can be extracted from the slope,

$$C \ln 10 = -\frac{\partial Q}{\partial \mathrm{pH}} \quad (12)$$

Thus, we can estimate the magnitude of the regulation interaction using the $1/R^2$ terms derived in the previous section. Where experimental titration data are not available, one may resort to theoretical models; the Tanford−Kirkwood theory, MC simulation, etc. This shall be the topic of the next section.

*Simulation Model.* In some recent studies, we have demonstrated how MC simulations can be used to predict protein−protein interactions in solution (*3*) as well as the titration behavior of an isolated protein in salt solution (*21*). Here, we shall give a brief introduction to these methods; for a more thorough survey, the reader may consult the references mentioned above.

The simulations are based on a simple dielectric continuum model and exploit the Protein Data Bank to provide a detailed structural description of the protein. The protein is treated either in full atomic detail, "atomistic model", or in a simplified version, where we represent each amino acid as a sphere, "the amino acid model". The aqueous solvent is treated as a structureless continuum described by the dielectric constant $\epsilon_r$ equal to that of pure water. The ions in the surrounding salt solution are described by charged, hard spheres allowed to move in any direction within a spherical cell enclosing the system of interest, see Figure 1.

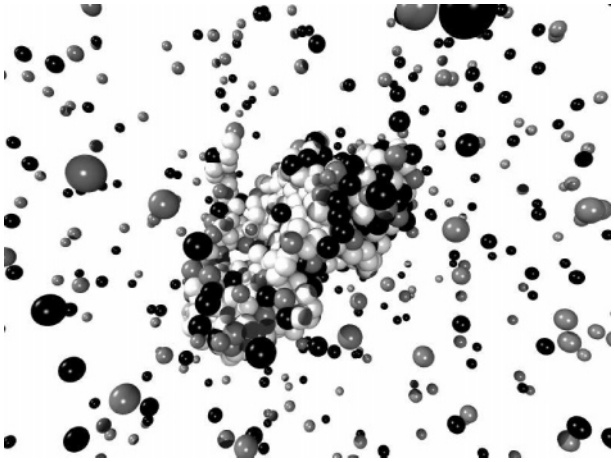

FIGURE 1: Schematic picture of the model system with the protein and salt solution enclosed in a cell.

Some of the simulations are performed for *two* proteins in a spherical cell. The same type of interactions are included, but now the two proteins are allowed to translate and rotate as well. From these simulations, we can calculate the free energy of interaction between the proteins.

In the amino acid model, each residue is replaced with a single sphere located at a center-of-mass of the residue according to the crystal structure and the radius is adjusted, so that the total protein volume is equal to that of the protein in full atomic detail. This amounts to an average amino acid radius of around 3.5 Å. The degree of protonation for each amino acid is affected by pH and by the potential produced by all other charges in the system. This has been incorporated into the simulations via a titration scheme, where protons are allowed to exchange between sites in the protein and the surrounding solution. The trial energy for such an exchange is calculated according to

$$\Delta U = \Delta U_{\mathrm{el}} \pm (\mathrm{pH} - \mathrm{p}K_0)\ln 10$$

where $\Delta U_{\mathrm{el}}$ is the change in electrostatic energy, p$K_0$ is the dissociation constant of the isolated amino acid, (+) applies when protonating an amino acid, and (−) applies when deprotonating an amino acid. Sites on the protein are selected randomly as is the proton (a positive charge) in the salt solution, when deprotonating the proton is inserted at a random position. Thus, during simulation, the protein charge will respond to changes in the electrostatic surroundings, which of course will be more important when pH ≈ p$K_0$. Note that, because the ionized residues are located near the surface, we have assumed a relatively high dielectric response from the surroundings. This allows us to use a uniform dielectric permittivity for the whole system equal to the value of pure water. Naturally, this assumption becomes less applicable for charges buried in the protein interior where the dielectric response may be smaller; in such cases, more sophisticated models should be utilized.

The total interaction energy for the system is written as a sum of contributions from electrostatics and hard-core repulsions

$$\beta U_{\mathrm{tot}} = \sum_{i,j\in p,s}\left(l_{\mathrm{B}}\frac{q_i q_j}{r_{ij}} + u_{ij}^{\mathrm{hs}}\right) \qquad i \neq j \qquad (13)$$

Table 1: Titrating Residues in the Investigated Proteins[a]

| protein | residues | Asp | Glu | His | Tyr | Lys | Cys[b] | Arg |
|---|---|---|---|---|---|---|---|---|
| p$K_0$ | | 4.0 | 4.4 | 6.3 | 9.6 | 10.4 | 10.8 | 12.0 |
| smMLCK (*16*) | 19 | 0 | 0 | 1 | 0 | 2 | 0 | 3 |
| calbindin $D_{9k}$ (*17*) | 75 | 4 | 13 | 0 | 1 | 10 | 0 | 0 |
| calmodulin (*16*) | 142 | 16 | 19 | 1 | 2 | 5 | 0 | 6 |
| hisactophilin (*18*) | 118 | 6 | 7 | 31 | 3 | 9 | 1 | 1 |
| M-m-CoA mutase (*19*) | 726 | 47 | 51 | 12 | 22 | 36 | 2 | 43 |
| lysozyme (*20*) | 129 | 7 | 2 | 1 | 3 | 6 | 0 | 11 |

[a] The dissociation constants for the isolated amino acids are given in the second line and the corresponding p$K_0$ for C and N termini are 3.8 and 7.5, respectively. [b] Only cysteines not engaged in sulfide bridges can titrate.

where the indexes $i$ and $j$ refer to salt ($s$) and protein ($p$) particles, separated by the distance $r_{ij}$. The hard-core term, $u_{ij}^{\mathrm{hs}}$ is ∞ for $r_{ij} < \sigma_i + \sigma_j$ and zero otherwise.

The model system is solved using the traditional Metropolis MC method (*22*), performed in a semicanonical ensemble. This means that the salt particles, positive or negative hard spheres, are subject to random displacement in the surrounding solution, while "protons", i.e., positive ions, can exchange between the solution and titrating groups on the protein. The whole system, including protein(s) and all ions, is electroneutral. The results from the simulation are the average charge on each titrating group and the distribution of co- and counterions around the protein. To calculate the response function, i.e., the protein capacitance, we will also calculate the protein average net charge, $\langle Q\rangle$, and the averaged squared net charge, $\langle Q^2\rangle$.

Again, we stress that MC simulation is just one of many methods that can be used to estimate capacitances; Equation 6 holds for any model.

## RESULTS

Using MC simulation, we have calculated the capacitance for a number of proteins with different characteristics in terms of number and type of residues (see Table 1). Unless otherwise stated, we have used a salt concentration of 70 mM and a protein concentration of 0.7 mM. This choice of conditions allows us to treat very large protein complexes with more than 1000 residues. Figure 2a shows the capacitance for calbindin $D_{9k}$ derived from the experimental titration curve (*21*, *23*) as well as from the atomistic and the amino acid model. The two models give virtually identical results, and below pH 9, the agreement with experimental data is very good. The discrepancy at high pH could be due to a minor unfolding of the protein; this would decrease the internal electrostatic perturbation and, as seen, shift capacitances toward the ideal curve. The main difference from the ideal capacitance curve is a strong broadening of two peaks corresponding to the response from acidic and basic residues, respectively.

Calmodulin is another calcium-binding protein, and its capacitance has the same qualitative appearance as calbindin. Both proteins have a large number of Asp/Glu residues giving rise to a large capacitance at pH 4. They also have a large portion of Lys/Arg resulting in a second peak at pH 11−12. Figure 2b shows the capacitance for calmodulin and for a small positively charged peptide from smooth muscle myosine light-chain kinase (smMCLK). The capacitance for the peptide is essentially zero below pH 10, while it peaks

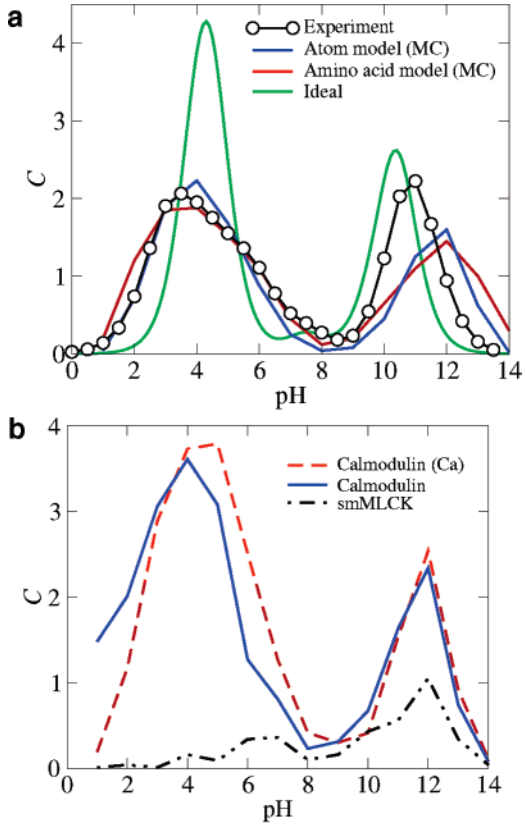


FIGURE 2: (a) Simulated, ideal, and measured [Kesvatera et al. (*21*, *23*)] capacitances for calbindin $D_{9k}$ as a function of pH. pI for calbindin is approximately 4.2. (b) Simulated (atomic model) capacitances for smMLCK, calmodulin (calcium free), and calmodulin with four calcium ions bound. pI for calmodulin is approximately 3.9.

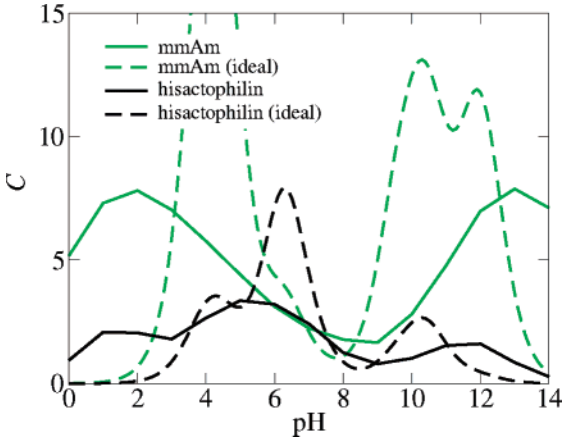


FIGURE 3: Simulated (amino acid model) and ideal capacitances for hisactophilin and methylmalonyl-CoA mutase (mmAm) as a function of pH. pI for hisactophilin is 7.3, and pI for methylmalonyl-CoA mutase is 5.2.

around pH 12 because of lysine and arginine residues. This maximum is much smaller than for calmodulin, but for the specific capacitance, i.e., $C_{sp} = C/N_{res}$, the situation is reversed.

The protein hisactophilin is of the same size as calbindin and calmodulin, but it has a slightly different capacitance curve, see Figure 3. Hisactophilin contains 31 histidine residues, which is reflected in a broad maximum for $C_{Hisacto}$ at pH 5−6. Because of the high positive charge of hisactophilin at acidic conditions (+28 at pH 3 and +23 at pH 4),

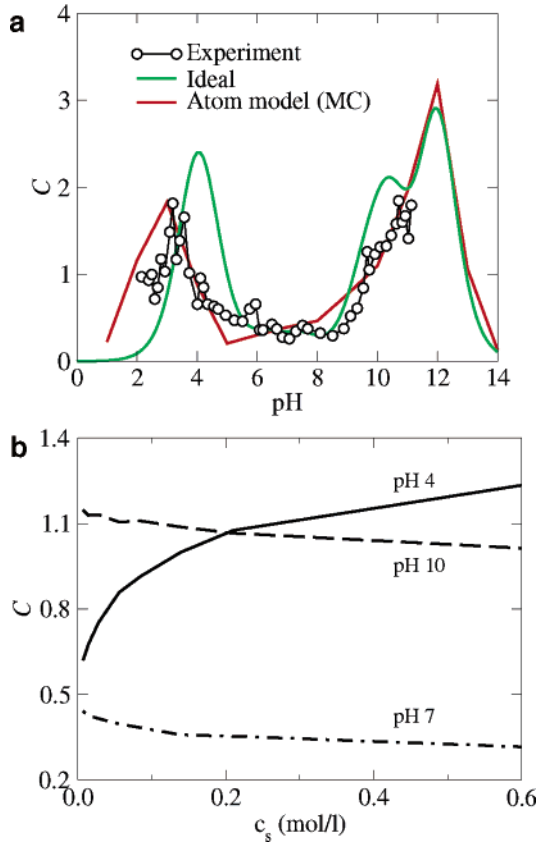


FIGURE 4: (a) Simulated, ideal, and measured capacitances for lysozyme. Experimental data are taken from Sakakibara and Hamaguchi (*26*). (b) Simulated capacitance for lysozyme (atomistic model) at different pH and salt concentrations.

the maximum is shifted downward. The isoelectric point found from the simulations is 7.3 in perfect agreement with experimental estimates (*24*). The relatively high capacitance of hisactophilin at physiological pH suggests that charge regulation may be of biological importance, for example, when coupling actin skeleton to negatively charged plasma membranes (*25*). In general, histidine-rich molecules are likely to have high capacitances around pH 7, thus making them good candidates for *in vivo* charge regulation.

The capacitance increases with protein size or more correctly with the number of titratable groups. Figure 3 also shows the capacitance for chain A in methylmalonyl-CoA mutase, which consists of more than 700 amino acids. The protein can achieve a very high net charge (+14 at pH 4 and −26 at pH 10) and a significant capacitance at extreme pH's. The isolelectric point is 5.2.

Lysozyme is another well-studied protein, and from the measured titration curve (*26*), we have extracted capacitances and, as shown in Figure 4a, agreement with the simulation is reasonable. Salt particles influence the capacitance (Figure 4b), but it is much less pronounced than the pH dependence. The salt effect is rather complex because it is governed by several mechanisms. In general, the effect of salt is to screen the electrostatic interactions, and hence, capacitances ought to approach their ideal values. However, the detailed charge distribution of the protein will modulate this effect. From this, it is difficult to derive any general statements because the balance depends not only on pH but also on the protein sequence and structure.

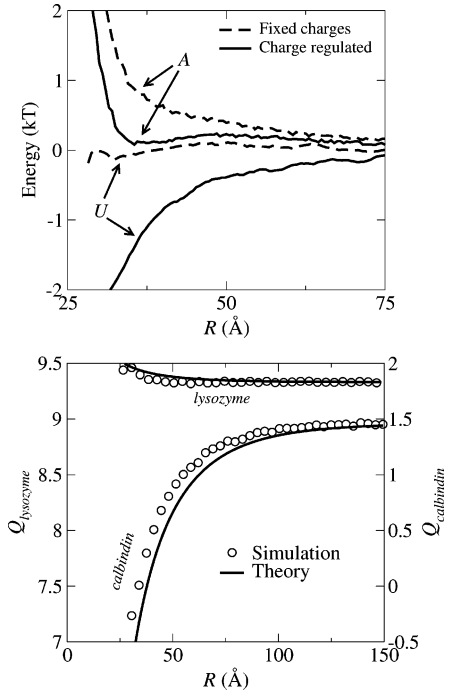


FIGURE 5: (a) Simulated energy ($U$) and free energy ($A$) of the interaction between calbindin and lysozyme at pH 4 for a protein model with fixed charges and one with charge regulation. The amino acid model is used, and the salt concentration is 6 mM. (b) Variation of the net charge of calbindin and lysozyme as a function of their separation. Circles represent simulated data based on the amino acid model, and lines are calculated from the induced charge cf. eq 5. The pH is 4, and the salt concentration is 6 mM.

The electrostatic interaction between two proteins will, at long distances, be dominated by the direct Coulomb interaction provided that the net charge, $Q$, is sufficiently different from zero. The induced interactions will play an important role only for protein−protein interactions at pH values close to the isoelectric point of one of the proteins; this can be seen from eq 6. We shall now illustrate this with an (artificial) example, where calbindin is interacting with lysozyme. Figure 5a shows the simulated free energy of interaction between the two proteins at pH 4, which is close to the isoelectric point for calbindin. At contact, there is a difference in the interaction energy of 1 kT between a model with fixed charges compared to a situation where the proteins are free to adjust their charges.

This difference between the two models is mainly due to the interaction between the induced charge in calbindin and the permanent charge in lysozyme. This is a typical result, and significant effects from charge regulation can be expected when one of the interacting proteins has a large net charge and the other has a large capacitance. Experimentally, this is confirmed by Zydney and Pujar (*9*), who were able to separate proteins by charge regulation at pH with high capacitances.

Following eq 6, we can approximate the difference between the fixed and regulated case as

$$\beta(A_{reg}(R) - A_{fix}(R)) = \beta\Delta A(R) = -\frac{l_B^2 e^{-2\kappa R}}{2R^2}(C_{calb}C_{lys} + C_{lys}Q_{calb}^2 + C_{calb}Q_{lys}^2) \quad (14)$$

where we have replaced the Coulomb interaction with a simple screened version to approximately account for the effect of salt. Figure 6 shows a perfect agreement between the simulated free-energy difference and the calculated one according to eq 14. Therefore, with minimal effort, eq 14 can be applied to existing models, for example, the DLVO approximation, so as to account for the induced charge interaction.

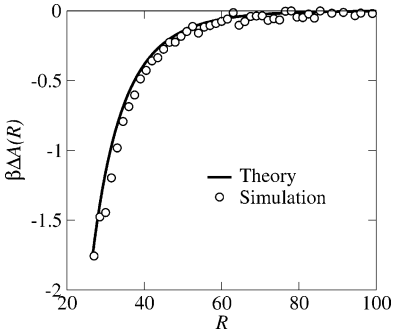


FIGURE 6: Difference in the free energy of interaction between calbindin and lysozyme at pH 4, with 6 mM salt for a protein model with charge regulation and one with fixed charges. Symbols denote the simulated difference (see Figure 5), and the solid line is obtained from eq 14 with $Q_{calb} = 1.46$, $C_{calb} = 2.23$, $Q_{lys} = 9.33$, $C_{lys} = 0.88$, and $1/\kappa = 39$ Å.

An interesting result is that, despite the fact that both calbindin and lysozyme are positively charged when isolated at pH 4, there is still an attractive electrostatic interaction between the two. Such an attraction could of course be due to charge−dipole and/or dipole−dipole interactions, but in the present case, the main contribution to the interaction free energy comes from the induced charges. This is further demonstrated in Figure 5b, where one can follow how the net charge of calbindin changes from +1.5 at infinite separation to −0.5 at contact between calbindin and lysozyme.

## DISCUSSION

We have derived an expression for the protein charge capacitance and showed how it appears as a response to an externally applied potential. The same capacitance also enters the expression for the free energy of interaction between two proteins allowed to regulate their charges. The induced interaction coming from a charge regulation mechanism can be important if one of the proteins is close to its isoelectric point, while the other carries a net charge. Via the presented formalism, existing models for protein−protein or protein−membrane interactions can be easily improved to correctly describe the induction interaction. Predictions of interaction free energies and induced protein charges are in excellent agreement with MC simulations that represent the exact theoretical solution.

The protein charge capacitance, $C$, can be obtained from measured titration curves and from any theoretical model able to predict the protein charge; our simple continuum simulations for the protein protonation status reproduce the experiment very well.

The capacitance varies with pH, and its magnitude is related to the number of titratable groups in a protein. Typically, $C$ will be large at pH values in the neighborhood of the p$K_a$ values of titrating residues, although the capacitance maximum can be shifted one or two pH units from the ideal maximum. The capacitance curve will also be

broadened because of interactions within the protein. This means that, in a protein with many aspartates and/or glutamates, the capacitance will have a maxium around pH 4, while a large number of histidines will lead to a maximum at pH $\approx$ 6 and similar for the basic residues.

## REFERENCES


1. Allahyarov, E., Löwen, H., Hansen, J. P., and Louis, A. A. (2002) Discrete charge patterns, coulomb correlations, and interactions in protein solutions, *Europhys. Lett. 57*, 731−737.
2. Carlsson, F., Malmsten, M., and Linse, P. (2001) Monte Carlo simulations of lysozyme self-association in aqueous solution, *J. Phys. Chem. 105*, 12189−12195.
3. Lund, M., and Jönsson, B. (2003) A mesoscopic model for protein−protein interactions in solution, *Biophys. J. 85*, 2940−2947.
4. Striolo, A., Bratko, D., Wu, J. Z., Elvassore, N., Blanch, H. W., and Prausnitz, J. M. (2002) Forces between aqueous nonuniformly charged colloids from molecular simulation, *J. Chem. Phys. 116*, 7733−7743.
5. Kirkwood, J. G., and Shumaker, J. B. (1952) Forces between protein molecules in solution arising from fluctuations in proton charge and configuration, *Proc. Natl. Acad. Sci. U.S.A. 38*, 863−871.
6. Carnie, S. L., and Chan, D. Y. C. (1993) Interaction free energy between plates with charge regulation: A linearized model, *J. Colloid Interface Sci. 161*, 260−264.
7. Carnie, S. L., Chan, D. Y. C., and Gunning, J. S. (1994) Electrical double layer interaction between dissimilar spherical colloidal particles and between a sphere and a plate: The linearized Poisson−Boltzmann theory, *Langmuir 10*, 2993−3009.
8. Pujar, N. S., and Zydney, A. L. (1997) Charge regulation and electrostatic interactions for a spherical particle in a cylindrical pore, *J. Colloid Interface Sci. 192*, 338−349.
9. Zydney, A. L., and Pujar, N. S. (1998) Protein transport through porous membranes: Effects of colloidal interactions, *Colloids Surf., A 138*, 133−143.
10. Menon, M. K., and Zydney, A. L. (2000) Determination of effective protein charge by capillary electrophoresis: Effects of charge regulation in the analysis of charge ladders, *Anal. Chem. 72*, 5714−5717.
11. Bowen, W. R., and Williams, P. M. (1996) The osmotic pressure of electrostatically stabilized colloidal dispersions, *J. Colloid Interface Sci. 184*, 241−250.
12. Ståhlberg, J., Appelgren, U., and Jönsson, B. (1995) Electrostatic interactions between a charged sphere and a charged planar surface in an electrolyte solution, *J. Colloid Interface Sci. 176*, 397−407.
13. Ståhlberg, J., and Jönsson, B. (1996) Influence of charge regulstion in electrostatic interaction chromatography of proteins, *Anal. Chem. 68*, 1536−1544.
14. Jönsson, B., and Ståhlberg, J. (1999) The electrostatic interaction between a charged sphere and an oppositely charged planar surface and its application to protein adsorption, *Colloids Surf., B 14*, 67−75.
15. Bratko, D., Woodward, C. E., and Luzar, A. (1991) Charge fluctuation in reverse micelles, *J. Chem. Phys. 95*, 5318.
16. Meador, W. E., Means, A. R., and Quiocho, F. A. (1992) Target enzyme recognition by calmodulin: 2.4 Å structure of a calmodulin−peptide complex, *Science 257*, 1251−1255.
17. Szebenyi, D. M. E., and Moffat, K. (1986) The refined structure of vitamin D-dependent calcium-binding protein from bovine intestine. Molecular details, ion binding, and implications for the structure of other calcium-binding proteins, *J. Biol. Chem. 261*, 8761−8777.
18. Habazettl, J., Gondol, D., Wiltscheck, R., Otlewski, J., Schleicher, M., and Holak, T. A. (1992) Structure of hisactophilin is similar to interleukin-1b and fibroblast growth factor, *Nature 359*, 855−858.
19. Mancia, F., and Evans, P. R. (1998) Conformational changes on substrate to methylmalonyl coa mutase and new insights into the free radical mechanism, *Structure 6*, 711−720.
20. Ramanadham, M., Sieker, L. C., and Jensen, L. H. (1990) Refinement of triclinic lysozyme: II. The method of stereochemically restrained least squares, *Acta Crystallogr., Sect. B 46*, 63−69.
21. Kesvatera, T., Jönsson, B., Thulin, E., and Linse, S. (1999) Ionization behaviour of acidic residues in calbindin $D_{9k}$, *Proteins 37*, 106−115.
22. Metropolis, N. A., Rosenbluth, A. W., Rosenbluth, M. N., Teller, A., and Teller, E. (1953) Equation of state calculations by fast computing machines, *J. Chem. Phys. 21*, 1087−1097.
23. Kesvatera, T., Jönsson, B., Thulin, E., and Linse, S. (2001) Focusing of the electrostatic potential at ef-hands of calbindin $D_{9k}$. Titration of acidic residues, *Proteins 45*, 129−135.
24. Hanakam, F., Eckerskorn, C., Lottspeich, F., Müller-Taubenberger, A., Schäfer, W., and Gerisch, G. (1995) The pH-sensitive actin-binding protein hisactophilin of dictyostelium exists in two isoforms which both are myristoylated and distributed between plasma membrane and cytoplasm, *J. Biol. Chem. 270*, 596−602.
25. Hanakam, F., Gerisch, G., Lotz, S., Alt, T., and Seelig, A. (1996) Binding of hisactophilin I and II to lipid membranes is controlled by a pH-dependent myristoyl-histidine switch, *Biochemistry 35*, 11036−11044.
26. Sakakibara, R., and Hamaguchi, K. (1968) Structure of lysozyme, *J. Biochem. 64*, 613−618.


BI047630O